Paper

Transient Nature of Argon and Molecular Gas-Seeded Argon Inductive Thermal Plasmas in Pulse Amplitude Modulation Approach

M.M. Hossain* Non-member
Yasunori Tanaka* Member
Tadahiro Sakuta*

In the present work, a high power (30 kW), atmospheric pressure inductive thermal plasma has been diagnosed both theoretically and experimentally in pulse amplitude modulation approach with Ar, Ar-CO_2, Ar-N_2, and Ar-O_2 as working gases (100 lpm argon and 2.5 lpm molecular gas). Simulation has been carried out using a two-dimensional local thermodynamic equilibrium (LTE) code for the same torch and operating conditions as that of experiment. Calculating the so-called response times from both simulated and experimental temporal radiation intensity of ArI at 751 nm, a rigorous and comprehensive comparative discussion has been made for a shimmer current level (SCL), the ratio of lower to higher level of current pulse, varying from 40%–100%. The measured temperature is also compared with the calculated apparent temperature. In spite of some discrepancies (at lower SCL) with the magnitude of response times of experimental and simulated plasma at the instant of on-pulsing transition, similar trend of those have been observed. These results will help to clear the understanding of transient performance of the concerned gases and equilibrium phenomena.

Keywords: pulse-modulated inductive thermal plasma, SCL, radiation intensity, response-time, temperature variation

1. Introduction

Inductive thermal plasma, a contamination free highly radiative plasma source, has been found widespread laboratory and industrial applications. Even though, some applications of inductive plasma [1] are already well established, optimization and automatic control of discharge are the forefront of current research activities. Since 1961 after Reed [2], a significant advancement of inductive plasma technology has been achieved. A huge number of works, both experimental and theoretical has been published that concerned the steady state plasma discharge. A few researchers have paid attention to the transient plasma nature following a sudden power interruption [3]~[5]. Ishigaki *et al* [6] and then Sakuta *et al* [7] first reported the repetitive pulsing discharge, which is termed Pulse-Modulated Inductive Thermal Plasma (PMITP). Pulse amplitude modulation of coil current, a new edition in inductive discharge, especially at high power and pressure, offers time and amplitude domain control of inductive discharge. It has been found very suitable for temporal and transient plasma studies. The concept of pulse-amplitude modulation of RF-coil current and its attractive and unique features are described elaborately in our previous publication [8] [9]. The experimental plasma reactor system of our laboratory has the following outstanding features: (i) solid state device, MOSFET employed inverter-feed pulse amplitude modulated coil current, (ii) this is a high power (maximum 50 kW) system works under a wide range of pressure (soft vacuum to 0.13 MPa), and (iii) as this system can work for a wide range of gas flow, thus, the transient

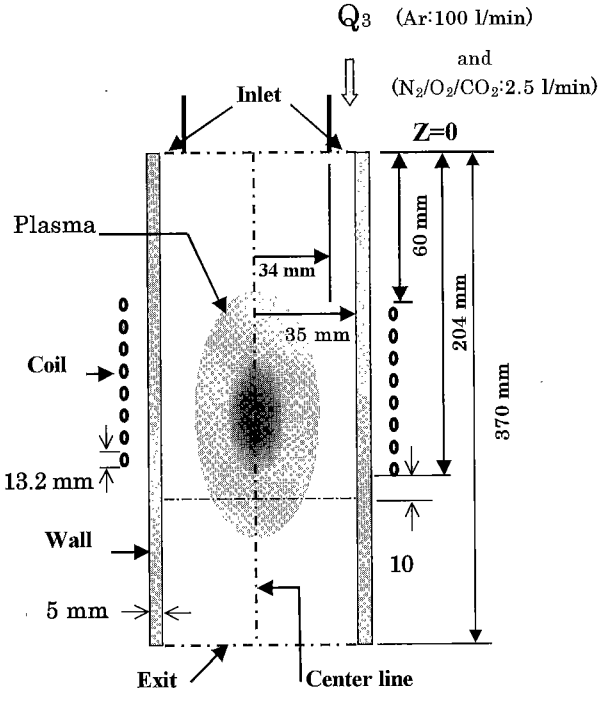

Fig. 1. Schematic diagram of the PMITP torch

* Department of Electrical & Electronic Engineering, Kanazawa University
2-40-20, Kodatsuno, Kanazawa 920-8667

nature of different plasma gases or their mixtures can be analyzed effectively. The periodic change of density and velocity of plasma species and successive extremely high and low heat produced in accord with pulsing current/power might have promising aspects in material processing such as surface hardening, synthesis of fine powders and plasma coating of materials.

It is aimed here to study the transient behavior of Ar, Ar-CO_2, Ar-N_2, and Ar-O_2 plasmas both experimentaly and theoretically and a comaparative discussion is made to interprete the differences between two approaches. Measuring/calculating the temporal radiation intensity at 751 nm of ArI, the response times are estimated/calculated. The spatial temperature profiles are also calculated.

2. Simulation Details

2.1 Assumption and Governing Equations

In this work, the plasma is assumed to be optically thin and electron temperature is equal to that of the neutral particles. The flow is assumed to be two-dimensional, steady, laminar, and axisymmetric with negligible viscous dissipation. Under these assumptions, the present model solves the time-dependent conservation equations along with the vector potential form of Maxwell's equations. The governing conservation equations are as follows:

Mass conservation:

$$\frac{\partial \rho}{\partial t}+\frac{\partial(\rho u)}{\partial z}+\frac{1}{r}\frac{\partial(r\rho v)}{\partial r}=0 \quad \cdots\cdots (1)$$

Momentum conservation:

Axial momentum:

$$\rho\frac{\partial u}{\partial t}+\rho u\frac{\partial u}{\partial z}+\rho v\frac{\partial u}{\partial r} = -\frac{\partial p}{\partial z}+2\frac{\partial}{\partial z}\left(\mu\frac{\partial u}{\partial z}\right) +\frac{1}{r}\frac{\partial}{\partial r}\left[r\mu\left(\frac{\partial u}{\partial r}+\frac{\partial v}{\partial z}\right)\right]+F_z \quad \cdots\cdots (2)$$

Radial momentum:

$$\rho\frac{\partial v}{\partial t}+\rho u\frac{\partial v}{\partial z}+\rho v\frac{\partial v}{\partial r} = -\frac{\partial p}{\partial r}+\frac{\partial}{\partial z}\left[\mu\left(\frac{\partial v}{\partial z}+\frac{\partial u}{\partial r}\right)\right] +\frac{2}{r}\frac{\partial}{\partial r}\left[r\mu\left(\frac{\partial v}{\partial r}\right)\right]+F_r \quad \cdots\cdots (3)$$

Energy conservation:

$$\rho\frac{\partial h}{\partial t}+\rho u\frac{\partial h}{\partial z}+\rho v\frac{\partial h}{\partial r} = \frac{\partial}{\partial z}\left(\frac{\lambda}{C_p}\frac{\partial h}{\partial z}\right)+\frac{1}{r}\frac{\partial}{\partial r}\left(r\frac{\lambda}{C_p}\frac{\partial h}{\partial r}\right)+P^\circ-R^\circ \quad \cdots\cdots (4)$$

Vector Potential Form of Maxwell's Equations:

Table 1. Operating conditions

Frequency = 450 kHz	Pulse on-time = 10 ms
Plate Power = 30 kW	Pulse off-time = 5 ms
Active plasma power =27 kW	Duty factor=67%
Pressure = 0.1 MPa	Flow-rate of Ar = 100 slpm
SCL(Shimmer Current Level;	(standard liter per minute)
a ratio of lower to higher	Flow-rate of $N_2/O_2/CO_2$
current level) = 40-100%	= 2.5 slpm

$$\frac{\partial^2 \boldsymbol{A_\theta}}{\partial z^2}+\frac{1}{r}\frac{\partial}{\partial r}\left(r\frac{\partial \boldsymbol{A_\theta}}{\partial r}\right)-\frac{\boldsymbol{A_\theta}}{r^2}=j\mu_0\sigma\omega\boldsymbol{A_\theta} \quad \cdots\cdots (5)$$

where t: time; ρ: mass density; μ: viscosity; λ: thermal conductivity; h: enthalpy; p: pressure; C_p: specific heat at constant pressure; F_z and F_r are axial and radial Lorentz forces respectively; u and v are axial and radial velocities; P°: volumetric Joule heating; R°: volumetric radiative loss; $\boldsymbol{A_\theta}$: phasor of vector potential; $\omega = 2\pi f$ (f is the frequency of coil current); μ_0: permeability of vacuum and j: complex factor.

2.2 Calculation Procedure Calculation is performed for an RF-ITP (Radio Frequency Inductive Thermal Plasma) torch whose schematics with the definitions of the parameters used in the simulation is illustrated in Fig. 1. In this calculation, only the sheath flow, which comprised of Ar, Ar-O_2, Ar-N_2 and Ar-CO_2, is considered. Table 1 outlines the operating conditions. Time step of each iteration, is 10 μs throughout the calculation. The calculations are carried out for a non-uniform grid system having 36 radial and 92 axial nodes. Using the SIMPLER algorithm of Patankar [10], the conservation equations and vector potential form of Maxwell's equation are solved for both steady and repetitive pulsation mode of coil current. The algorithm is based on control volume scheme for solving the transport equations of incompressible fluids considering the effect of temperature on density. For the details of the modeling readers are referred to Ref. (8).

2.3 Thermodynamic and Transport Properties The transport properties of Ar, O_2, N_2, and CO_2 gases required for simulation include viscosity, specific heat at constant pressure, electrical and thermal conductivity, mass density, and radiative loss coefficient. The transport properties, which are functions of temperature, were calculated under thermal equilibrium conditions using Chapman-Enskog first approximation of Boltzmann Equation [11].

2.4 Boundary Conditions The boundary conditions adapted in this work are as follows:

(i) Inlet: Gas temperature and axial gradient of vector potential are set to 300 K and zero respectively. (ii) Center line: Vector potential and radial gradients of all fields are set to zero. (iii) Wall: Temperature is set to 350 K, and (iv) Exit: Axial gradients of all fields are set to zero.

2.5 Simulated Results Figure 2 presents the spatial distribution of plasma temperature predicted over a pulsing cycle. This figure clearly describes the repetitive nature of pulse-modulated plasma. In

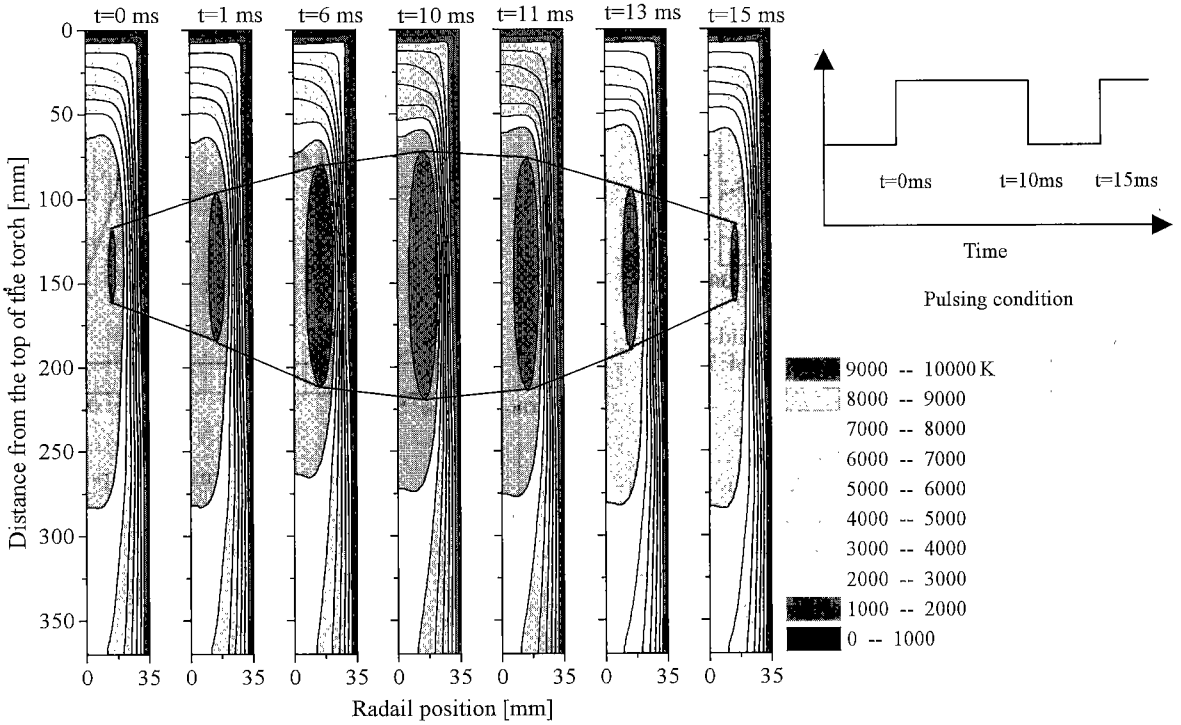

Fig. 2. Spatial distribution of temperature at some instants over a pulsing cycle at 70% SCL for Ar-N_2 PMITP

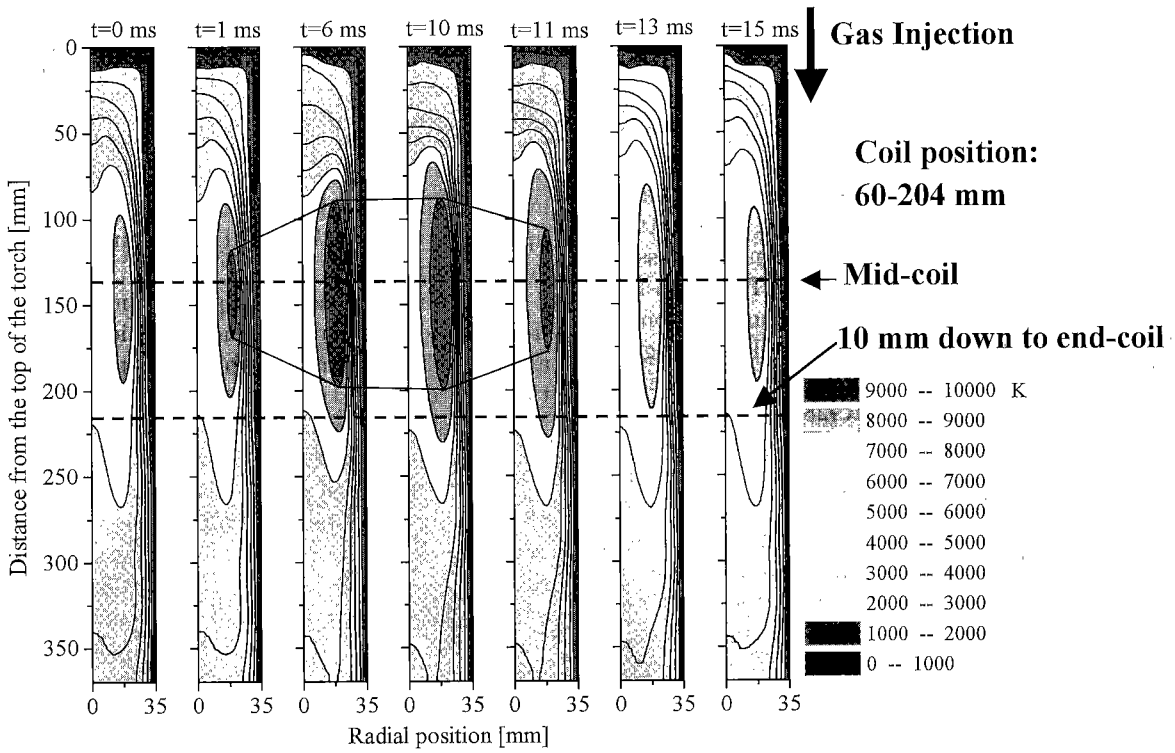

Fig. 3. Spatial distribution of temperature at some instants over a pulsing cycle at 70% SCL for Ar-CO_2 PMITP

this case, the working gas is Ar-N_2 (Ar: 100 lpm and N_2: 2.5 lpm), for 70% SCL, 67% duty factor (on-pulse time 10 ms) and at atmospheric pressure. It can be seen that at the end of off-pulse the high-temperature zones become narrower due to the scarce of effective plasma power and gradually becomes larger just after the on-pulse trigger. Figure 3 shows the spatial temperature field of Ar-CO_2 PMITP for the same operating conditions as those of Fig. 2. It can be found that temperature contours greatly suppressed during the off-pulse period compared with Ar-N_2 PMITP. This indicates the strong extinguishing charateristics of CO_2.

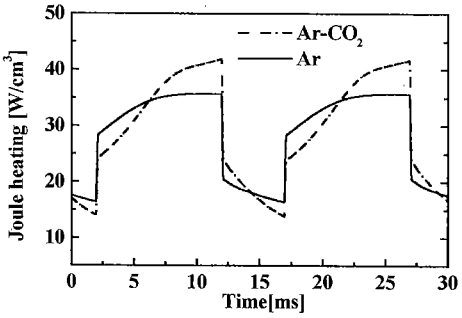

Fig. 4. Time evolution of Joule heating at mid-coil (z=132 mm) and r=17.5 mm, for an SCL of 76% and T_{on} = 10 ms, and T_{off} = 5 ms

In Figs. 2 and 3, the color bar representing the temperature has the dimension of K. Figure 4 describes the time evolution of Joule heating for Ar and Ar-CO_2 plasmas for an SCL of 76%, and flow rate of 100 slpm Ar and 2.5 slpm CO_2. It is observed from the figure that at 76% SCL, 2.4% addition of CO_2 increases the Joule heating by 20%, which results from the higher heat capacity and thermal conductivity of CO_2.

3. Comparative Discussion

3.1 Experimental and Spectroscopic Measurement The torch can be operated with a wide variety of plasma gases providing an extremely clean and effective thermal reaction environment. Figure 1 describes the schematic geometry and dimensions of the inductive plasma torch. The detailed reactor description and experimental setup will be found in Ref. (8). The plasma emission is taken by an optical system (camera) with a spatial resolution of 1 mm and transmitted through an optical fiber. The optical signal is passed into the monochromator through a slit. The emission intensity is then monochromated by the monochromator (JOBIN YVON HR-320) for the selected wavelength. The monochromated optical signal is then passed into the photomultiplier (Hamamatsu, R928) with a response time of 70 ns. This detected signal is stored by a multichannel oscilloscope (DL706E, Yokogawa Electric Co.) with minimum sampling time of 0.5 μs per address.

Table 1 outlines the discharge conditions. Using our spectroscopic measuring system, the temporal radiation intensity of ArI at 751 nm, 703 nm, and 714.7 nm together with the pulsing signal and modulated current waveform have been measured. And the response-times, which represent the dynamic plasma characteristics, have been estimated from the temporal radiation intensity for different SCL at two axial positions of the torch. Using two-line method (as described below) the time-dependent excitation temperature has been evaluated.

3.2 Calculation of Integrated Radiation Intensity Time-dependent plasma fields such as temperature, and integrated radiation intensity are calculated in a two-dimension space to compare with those of experiment. The plasma temperature is calculated solving the energy conservation equation and hence integrated

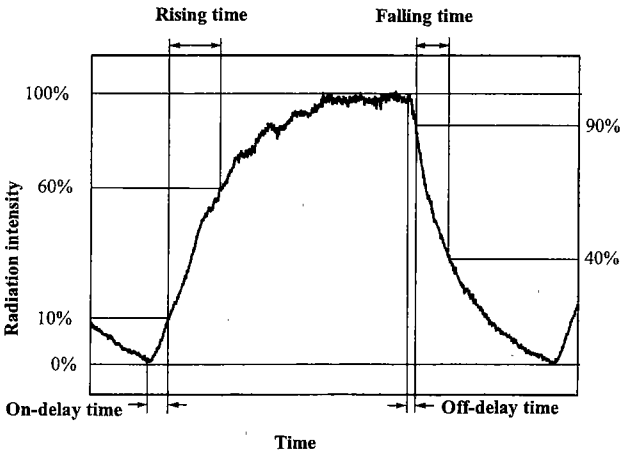

Fig. 5. Definitions of dynamic response times

radiation intensity for ArI at 751 nm is predicted from the temporal temperature distributions using the following equations:

$$I_z = 2\pi \int_0^{R_0} \varepsilon(T,r) r dr \cdots\cdots\cdots\cdots\cdots\cdots (6)$$

$$\varepsilon(T,r) = \frac{1}{4\pi} \frac{hcgAN(T)}{\lambda Z(T)} \exp\left(-\frac{E_n}{kT}\right) \cdots\cdots\cdots (7)$$

where I_z is the integrated radiation intensity at a particular axial position, ε is the emission coefficient, h is Planck's constant, c and λ are velocity and wavelength of light respectively, g is the statistical weight and A is the transition probability for spontaneous emission, $N(T)$ and $Z(T)$ are temperature-dependent particle density and internal partition function respectively, E_n is the upper energy level, k is the Boltzmann's constant and T is the temperature.

The so-called plasma response times are calculated from the temporal radiation intensities for various SCL at mid-coil and 10 mm down to the end-coil. The definitions of response times are clearly described in Fig. 5. The physical interpretation of those will be found in Ref. (8).

The apparent temperature predicted at mid-coil and 10 mm down to the end-coil position, using two-line method. The expression of apparent temperature is shown in Eq. (8). Symbols in Eq. (8) bear the same meaning as those of Eq. (7). In this calculation we have chosen atomic argon lines at 703 and 714.7 nm wavelength.

$$T_{appt} = \frac{E_2 - E_1}{k \ln\left(\frac{I_{z_1}\lambda_1 g_2 A_2}{I_{z_2}\lambda_2 g_1 A_1}\right)} \cdots\cdots\cdots\cdots\cdots (8)$$

3.3 Comparison Figure 6 presents the temporal radiation intensity of ArI at 751 nm for Ar-CO_2 plasma at mid-coil and 10 mm down to the end-coil. The SCL is 70%, on and off-time of pulsing signal are 10 and 5 ms respectively. It can be seen that the maximum deviation between measured and simulated radiation intensity occurs after approximately 5 ms of on-pulse trigger. Less

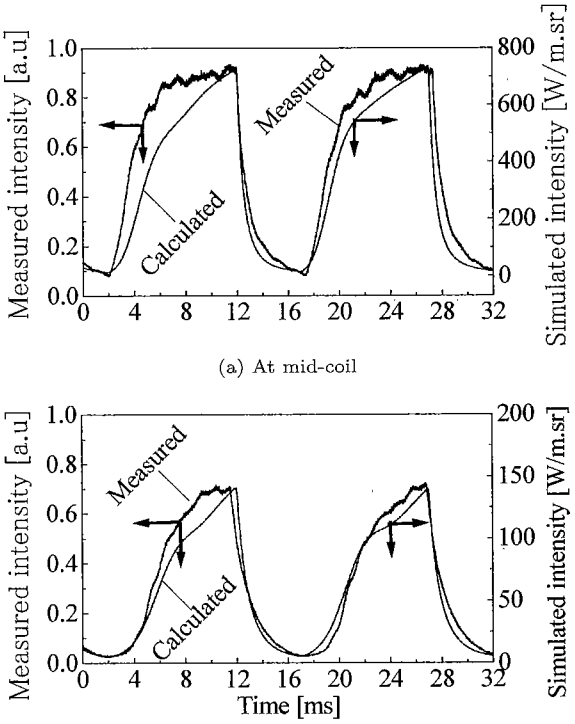

(a) At mid-coil

(b) At 10 mm down to the end-coil

Fig. 6. Comparison of measured and simulated radiation intensity of ArI at 751 nm for Ar-CO_2 PMITP at 60% SCL

discrepancy between simulated and experimental intensities is found at 10 mm down to the end-coil than that of at mid-coil. To describe the plasma reponse quantitatively, response times are calculated/estimated from the simulated/measured temporal radiation intensity. Figure 7 shows the plasma response times predicted from simulated and spectroscopically measured temporal radiation intensity of ArI at 751 nm for Ar, Ar-O_2, Ar-N_2, and Ar-CO_2 plasmas. Both in simulation and experiment, plasma response is found faster at higher SCL irrespective of axial position. However, discrepancies are observed between experimental and simulated results, especially, at lower SCL. Because at lower SCL, experimental PMITP strongly deviated from LTE ($T_e = T_h$), whereas, simulated PMITP is still in LTE state. During off-pulse at lower SCL, power input is at minimum level and hence temperature drops. The continued injection of cold gas through the sheath channel at insignificant power input enhances the cooling action of plasma. These two effects drive experimental PMITP at severe non-LTE ($T_e > T_h$) condition at lower SCL. Thus, the maximum deviations are observed at lower SCL. It is evident from Fig. 7 that, as well as the SCL moves towards 100%, the pulse-modulated plasma embraces the thermal equilibrium conditions. On the other hand, good agreement is observed between experimental and simulated results for Ar-CO_2 plasma. Figure 8 presents the maximum and minimum radiation intensities, tabulated from experimental and simulated temporal radiation intensities of ArI at 751 nm. Although, the maximum level of intensity does not change appreciably with SCL, the minimum level drops in a significant

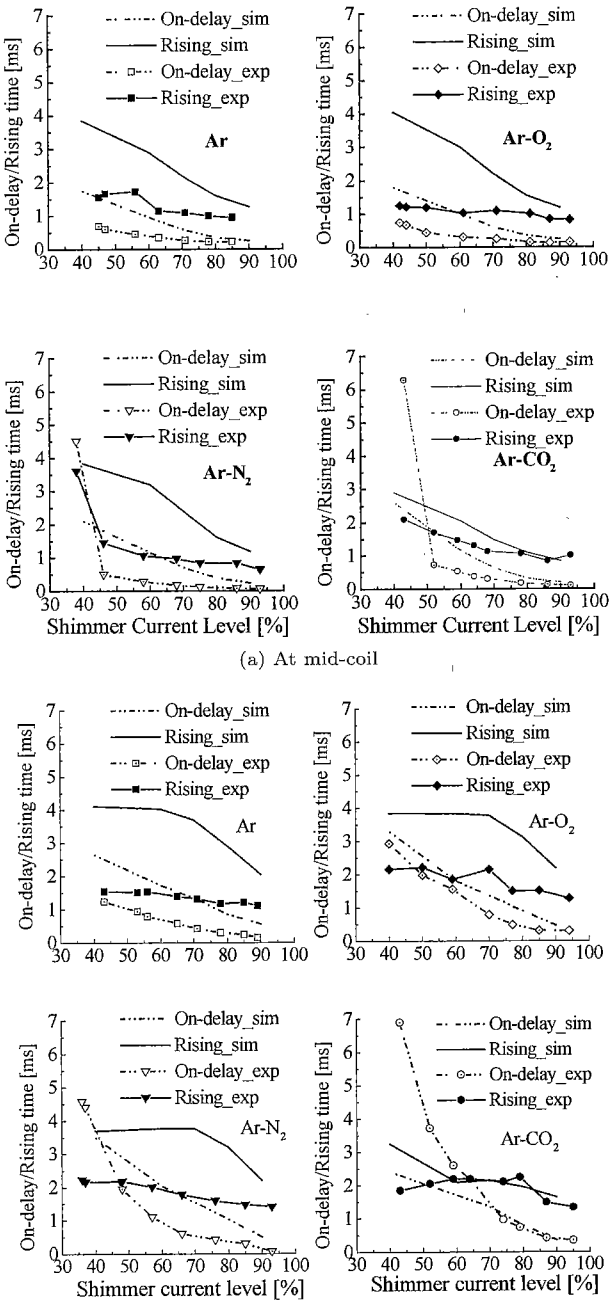

(a) At mid-coil

(b) At 10 mm down to the end-coil

Fig. 7. SCL dependence of simulated and experimental dynamic response times at 0.1 MPa pressure

extent at decreased SCL. This is because, a lower SCL means a bigger fluctuation of current as well as power, and hence the radiation intensity. The largest drop of minimum level takes place for Ar-CO_2 plasma that recalls the strong extinguishing nature of CO_2. A good agreement has been observed between experimental and simulated findings, especially, in case of Ar-CO_2 plasma. The measured time-dependent temperature is compared with the simulated apparent temperature in Fig. 9, for a SCL of 70%, and flow-rate of 100 lpm Ar and 2.5 lpm CO_2, at 10 mm down to the end-coil. This figure shows the similar trends of simulated and experimental temperature; however, the higher absolute value of temperature is found in experiment. The probable reason is

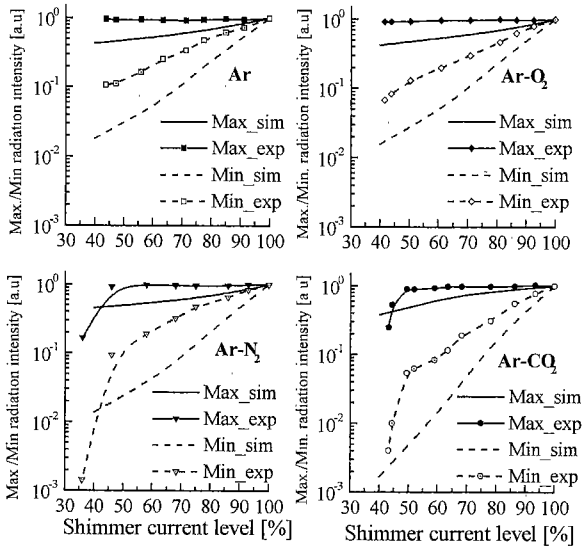

(a) At mid-coil

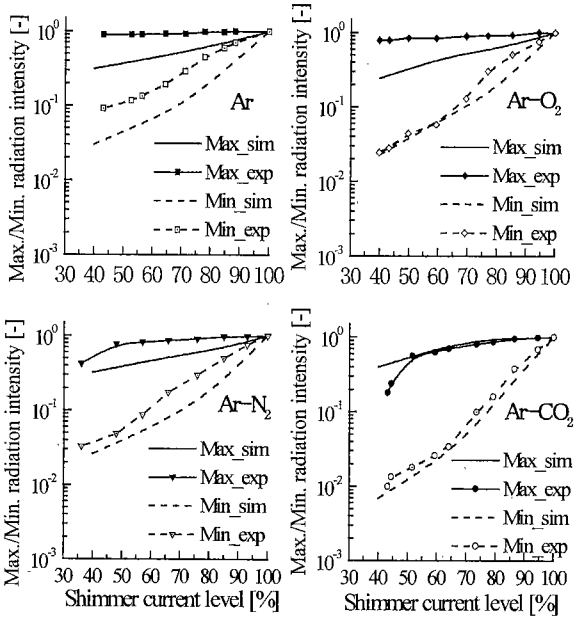

(b) At 10 mm down to the end-coil

Fig. 8. Comparison of the maximum and minimum levels of simulated and measured radiation intensity of ArI at 751 nm

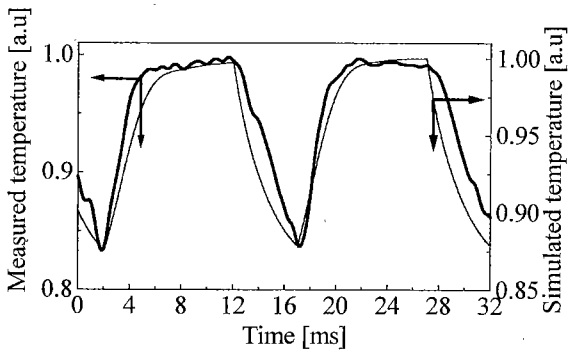

Fig. 9. Comparison of measured and simulated temperature at 10 mm down to the end-coil, for Ar-CO_2 plasma at 60% SCL and 0.1 MPa pressure

that experimental temperature corresponds the excitation temperature, which is close to electron temperature, whereas, simulated temperature corresponds the equilibrium temperature.

4. Conclusion

It is evident from the results that CO_2 has the strongest extinguishing nature than that of Ar, N_2, and O_2 which results from its thermal conductivity and heat capacity. Good agreements have been found between experimental and simulated response times at higher SCL, and for CO_2-admixed plasmas; however deviations are observed at lower SCL and for pure Ar plasma. The deviations between experimental and simulated finding result from the LTE assumption, and exclusion of detailed dissociation and charge transfer mechanisms in simulation.

Acknowledgment

The authors would like to thank Mr. M. Katayama for his cooperation in carrying out the experiment.

(Manuscript received Feb. 28, 2003,
revised June 19, 2003)

References

(1) M.I. Boulos, P. Fauchais, and E. Pfender: Thermal Plasmas-Fundamentals and Applications, Vol.1, Plenum, New York (1994)

(2) T.B. Reed: "Induction-Coupled Plasma Torch", *J. Appl. Phys.*, Vol.32, pp.821–824 (1961)

(3) P. Meubus: "Transient Conditions in Inductively Heated Plasmas: Thermodynamic Equilibrium and Temperature Measurements", *Can. J. Phys.*, Vol.60, pp.886–892 (1982)

(4) J.M. de Regt, Van der Mullen, and D.C. Schram: "Responses of the Electron Density and Temperature to the Power Interruption Measured by Thompson Scattering in an Inductively Coupled Plasma", *Phys. Rev.*, Vol.52, pp.2982–2987 (1995)

(5) F.H.A. Fey, W.W. Stoffels, J.A.M. van der Mullen, B. van der Sijde, and D.C. Schram: "Instantaneous and Delayed Responses of Line Intensities to Interruption of the RF Power in an Argon Inductively Coupled Plasma", *Spectrochim. Acta*, Vol.46B, pp.885–900 (1991)

(6) T. Ishigaki, X. Fan, T. Sakuta, T. Banjo, and Y. Shibuya: "Generation of pulse-modulated induction thermal plasma at atmospheric pressure", *Appl. Phys. Lett.*, Vol.71, pp.3787–3789 (1997)

(7) T. Sakuta, K.C. Paul, M. Katsuki, and T. Ishigaki: "Experimentally Diagnosed Transient Behavior of Pulse Modulated Inductively Coupled Thermal Plasma", *J. Appl. Phys.*, Vol.85, pp.1372–1377 (1999)

(8) M.M. Hossain, Y. Hashimoto, Y. Tanaka, K.C. Paul, and T. Sakuta: *IEEE Trans. Plasma Sci.*, Vol.30, pp.327–337 (2002)

(9) Y. Tanaka and T. Sakuta: "Stable Operation Region and Dynamic Behavior of Ar Pulse-Modulated Induction Thermal Plasma with Different Gases", *T. IEE Japan*, Vol.122-A, pp.469–478 (2002) (in Japanese)

(10) S.V. Patankar: Numerical Fluid Flow and Heat Transfer, Hemisphere, New York (1980)

(11) Y. Tanaka, K.C. Paul, and T. Sakuta: "Thermodynamic and Transport Properties of N_2/O_2 Mixture at Different Admixture Ratio", *T. IEE Japan*, Vol.120-B, pp.24–30 (2000)

M.M. Hossain (Non-member) was born on December 1, 1969. He received B.S. from Bangladesh University of Engineering and Technology, Dhaka in 1994. He received M.S. and Ph.D. from Kanazawa University in 2000 and 2003 respectively, in electrical engineering. He joined as a Lecturer in the Department of Electrical & Electronic Engineering, Bangladesh Institute of Technology, Chittagong, Bangladesh in April 1994. Currently he is an Assistant Professor of the same Department. His research interests include inductive plasma and its applications.

Yasunori Tanaka (Member) was born in Japan on November 19, 1970. He received the B.S., M.S. and Ph.D. degrees in elcetrical engineering from Nagoya University, Japan in 1993, 1995 and 1998 respectively. In April 1998 he was appointed Research Associate at Kanazawa University. He has been working as Associate Professor since August 2002 at same university. His research interests include the arc interruption phenomena and thermal plasma applications.

Tadahiro Sakuta was born on January 3, 1950 and died on January 26, 2003. He received the PhD degree from Department of Electrical Engineering, Nagoya University, Japan in 1980. In April 1981 he was appointed Research Associate at the same Department. Since April 1988 he had been working as an Associate Professor and then as a Professor in the Department of Electrical and Electronic Engineering, Kanazawa University. His research intersets included the diagnosis and applications of high-pressure thermal plasmas including induction plasma and circuit breaker arcs. Prof. Sakuta was affiliated with different scientific societies including IEEE, IEE of Japan.